OPTICA

Terahertz-wave decoding of femtosecond extreme-ultraviolet light pulses

I. Ilyakov,[1,†] N. Agarwal,[2,3,4,5,†] J.-C. Deinert,[1] J. Liu,[2] A. Yaroslavtsev,[2,6] L. Foglia,[7] G. Kurdi,[7] R. Mincigrucci,[7] E. Principi,[7] G. Jakob,[8] M. Kläui,[8] T. S. Seifert,[9,10] T. Kampfrath,[9,10] S. Kovalev,[1,13] R. E. Carley,[2,14] A. O. Scherz,[2] and M. Gensch[11,12,15]

[1]*Institute of Radiation Physics, Helmholtz-Zentrum Dresden-Rossendorf, Bautzner Landstr. 400, 01328 Dresden, Germany*
[2]*European XFEL, Holzkoppel 4, 22869 Schenefeld, Germany*
[3]*Max Planck Institute for the Structure and Dynamics of Matter, Luruper Chaussee 149, 22761 Hamburg, Germany*
[4]*Department of Physics, Universität Hamburg, Jungiusstraße 9, 20355 Hamburg, Germany*
[5]*Institute of Physics and Astronomy (IFA), Aarhus University, Ny Munkegade 120, 8000 Aarhus C, Denmark*
[6]*Department of Physics and Astronomy, Uppsala University, PO Box 516, 75120 Uppsala, Sweden*
[7]*Elettra-Sincrotrone Trieste S.C.p.A., 34149 Basovizza, Trieste, Italy*
[8]*Johannes Gutenberg University Mainz, Institute of Physics, Staudinger Weg 7, 55128 Mainz, Germany*
[9]*Department of Physics, Freie Universität Berlin, Arnimallee 14, 14195 Berlin, Germany*
[10]*Fritz Haber Institute of the Max Planck Society, Faradayweg 4-6, 14195 Berlin, Germany*
[11]*Institute of Optical Sensor Systems, DLR (German Aerospace Center), Rutherfordstr. 2, 12489 Berlin, Germany*
[12]*Institute of Optics and Atomic Physics, Technische Universität Berlin, Strasse des 17. Juni 135, 10623 Berlin, Germany*
[13]*e-mail: s.kovalev@hzdr.de*
[14]*e-mail: robert.carley@xfel.eu*
[15]*e-mail: michael.gensch@dlr.de*

In recent years, femtosecond extreme-ultraviolet (XUV) and x-ray pulses from free-electron lasers have developed into important probes to monitor processes and dynamics in matter on femtosecond-time and angstrom-length scales. With the rapid progress of versatile ultrafast x-ray spectroscopy techniques and more sophisticated data analysis tools, accurate single-pulse information on the arrival time, duration, and shape of the probing x-ray and XUV pulses becomes essential. Here, we demonstrate that XUV pulses can be converted into terahertz electromagnetic pulses using a spintronic terahertz emitter. We observe that the duration, arrival time, and energy of each individual XUV pulse is encoded in the waveform of the associated terahertz pulses, and thus can be readily deduced from single-shot terahertz time-domain detection. © 2022 Optica Publishing Group under the terms of the Optica Open Access Publishing Agreement

https://doi.org/10.1364/OPTICA.453130

1. INTRODUCTION

Ultrashort light pulses ranging from the extreme-ultraviolet (XUV) to the hard x-ray regime are available from several x-ray free-electron laser (XFEL) facilities worldwide [1]. The latest generation of these is based on superconducting radio-frequency (SRF) technology and provides pulses at repetition rates from the few 10 Hz to 100 MHz range [2,3], thereby enabling one to probe dynamics in materials, molecules, and atoms on all relevant time, length, and energy scales with excellent sensitivity [4–6]. However, despite this progress, the intrinsic and often unknown fluctuations of the x-ray pulse properties still do not allow one to realize the full potential of the many fascinating research opportunities.

In this paper, we present a novel concept to determine critical x-ray pulse parameters such as arrival time, pulse duration, and pulse energy changes. Our approach is based on the analysis of terahertz (THz) light pulses generated by the femtosecond x-ray/XUV pulses via optical rectification inside a broadband spintronic THz emitter (STE). Details of the experimental setup

are shown in Fig. 1. We show that the envelope of the x-ray/XUV pulse is encoded into the ultrashort photocurrent inside the x-ray-irradiated STE. By sampling and analyzing the full electric field of the concomitantly emitted THz pulse, we are able to retrieve information about the arrival time, duration, and energy of the original x-ray/XUV pulse. The advantage of our concept in comparison to other schemes to derive the arrival time [7–12], pulse duration [13–18], and pulse energy [19] is its simplicity, robustness, and potential to obtain all of these XUV/x-ray pulse properties from one single measurement. Our results also demonstrate optical rectification of XUV pulses with wavelengths one order of magnitude shorter than in all previous experiments [20–22].

2. EXPERIMENTAL SETUP

Our experiments were performed at the EIS-TIMEX beamline of the XUV free-electron laser FERMI in Trieste/Italy. As schematically shown in Fig. 1(a), the XUV pulses, generated by a
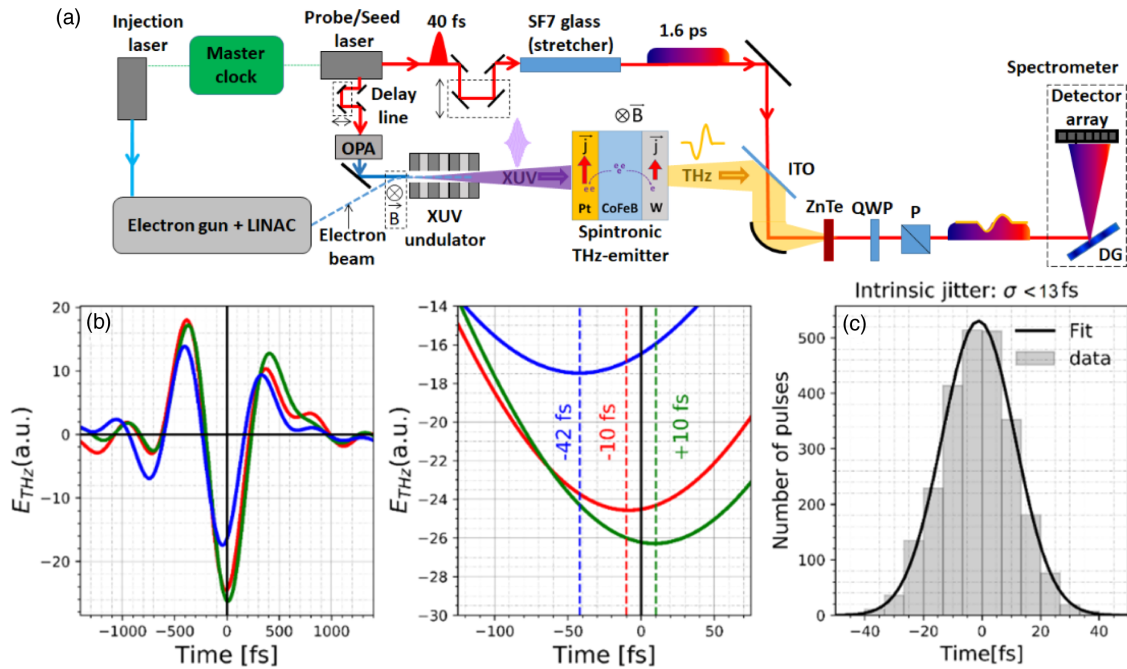
Fig. 1. Experimental setup as employed at the FERMI free-electron laser. (a) Schematic showing all relevant components of the seeded free-electron laser and implementation of the THz monitor concept, (b) plot of three THz pulses emitted from three subsequent XUV pulses with an average pulse energy of 20 μJ and wavelength of 20 nm, and (c) histogram showing the observed jitter of below 13 fs (rms) for the nominally intrinsically synchronized seeded x-ray pulses from the FERMI free electron laser.

high-gain harmonic-generation (HGHG) seeding scheme, were normally incident onto a purpose-built, large-area 10×10 mm^2 STE (TeraSpinTec GmbH) [23–25], which consists of a Pt(2 nm)|CoFeB(1.8 nm)|W(2 nm) tri-layer on a 500 μm thick z-cut sapphire substrate. The sample was magnetized in-plane by a constant magnetic field of 100 mT. The emitted THz pulse propagates in the forward direction through the sapphire substrate before entering free space.

The pulse energy of the XUV pulses could be adjusted up to 42 μJ per pulse. The experiments were performed with wavelengths of 20 and 29 nm and an estimated pulse duration of 30 and 35 fs, respectively. The repetition rate was 25 Hz. To operate the STE in the linear regime, the pump-beam diameter at the sample position was chosen to be 8 mm, thereby keeping the pump fluence below 0.1 mJ/cm^2 [24]. The emitted THz pulses were detected by a purpose-built single-shot detection scheme. The scheme is based on electro-optic encoding of a co-propagating THz electric-field waveform onto the frequency spectrum of the chirped optical probe pulse (1.6 ps, full-width half-maximum), and subsequent decoding by decomposing the probe beam into the frequency spectrum as shown in Fig. 1(a) (see [26,27] and Supplement 1 for details). The single-shot traces were additionally denoised by spectral filtering [27].

3. RESULTS

A. Arrival Time Monitoring

Figure 1(b) shows three consecutive THz pulses emitted from the STE upon impact of three subsequent XUV pulses. They exhibit not only different amplitudes, but as can be seen in the magnified view (right panel), differences in arrival time of only a few femtoseconds can clearly be observed. A histogram of the jitter

as determined by the arrival time monitor for 2500 subsequent XUV pulses is shown in Fig. 1(c). The typical arrival time jitter of FERMI observed in our measurement is below 13 fs (rms). Our results compare well with earlier jitter measurements performed at FERMI, which yielded values between 5.9 and 9.8 fs (rms) [12]. The slightly larger jitter observed in our scheme may stem from instabilities in the optical paths of our setup or from a slightly decreased precision of our measurement for lower XUV pulse intensities (see Supplement 1). Another possibility is that the jitter of the facility was simply larger during our measurements.

To characterize the robustness and reliability of our scheme, we artificially introduced periodic arrival time variations of the optical delay line between the common oscillator and seed laser optical parametric amplifier (OPA), thus altering the arrival time of the seed laser on the electron bunch [see Fig. 1(a)]. The results are presented in Fig. 2 where the determined arrival times for in total 600 subsequent pulses are plotted. A timing jitter of 10 fs can easily be detected with our arrival time monitor as can be seen in Fig. 2(b). The observed timing jitter for a delay line of 0 fs, corresponding to the intrinsic timing jitter of the FERMI FEL convolved with the precision of our arrival time monitor, is shown in Fig. 2(c). This particular measurement yields a timing jitter of below 13 fs (rms), as also shown as a histogram in Fig. 1(c).

B. Pulse Energy Monitoring

In the current understanding of STE operation, the absorbed FEL pulse triggers an ultrafast spin current into the nonferromagnetic layers where it is converted into a charge current by the inverse spin Hall effect. The amplitude of the emitted THz pulse [23,28] is expected to be a direct measure of the incident x-ray pulse energy for a constant pulse duration and shape. To put this idea to test, we took advantage of the sizeable pulse energy fluctuations of the
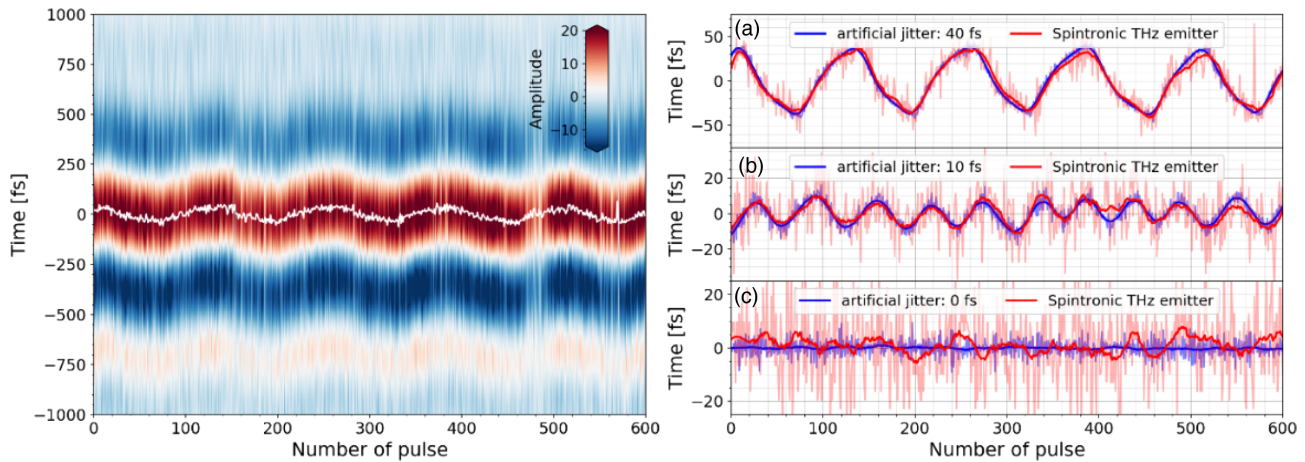
Fig. 2. Benchmarking of the scheme as arrival time monitor: 2D plot of the THz electric field for 600 consecutive pulses with artificial timing jitter of 40 fs (left, color coding represents field strength); white line represents the central peak of the THz waveform. (a) Corresponding line-out of the temporal position of the central maximum of the THz waveform for an artificial jitter of approximately 40 fs, (b) line-out for approximately 10 fs, and (c) line-out for 0 fs. The light blue line indicates artificially introduced arrival time variations, and the light red line denotes the observed arrival time jitter. The blue and red lines are smoothed values of the introduced and observed time jitters. The XUV wavelength for these measurements is 20 nm, pulse duration is 30 fs, and pulse energies vary between 5 μJ and 30 μJ.
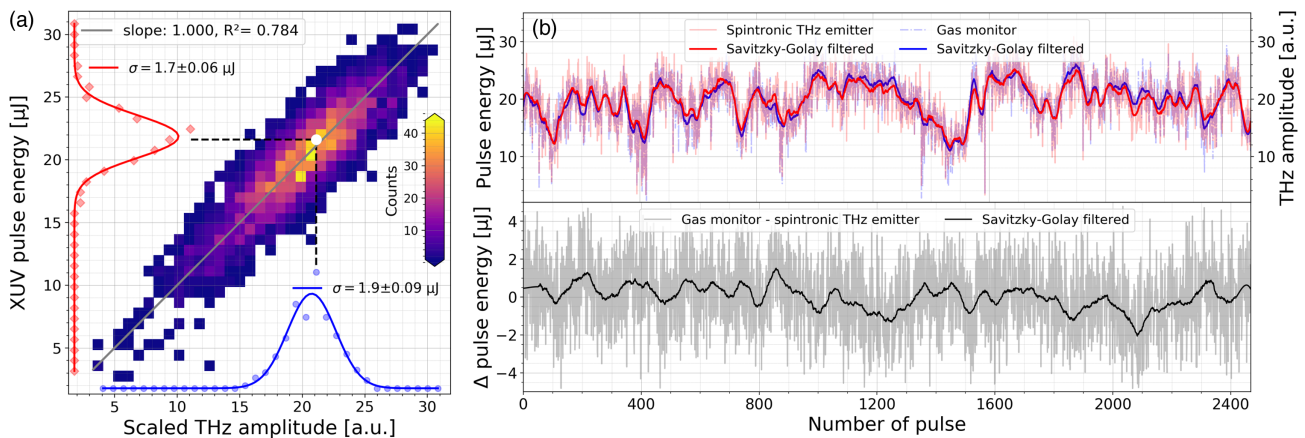

Fig. 3. THz amplitude and XUV pulse energy. (a) Correlation of the XUV pulse energy and THz amplitude over roughly 2500 pulses. R-squared of 0.784 is a statistical measure of the linear fit in gray. Correlation widths σ are fitted to be 1.7 μJ and 1.9 μJ, respectively, indicating a strong linear correlation between XUV pulse energy and scaled THz amplitude. (b) XUV pulse energy (blue) and THz amplitude (red) as a function of pulse number (top). Plotted difference between the reading from the gas monitor and the observed THz amplitude.

FERMI FEL. Figure 3(a) correlates the amplitude of the emitted THz pulses with the XUV pulse energy measured by the FERMI XUV pulse energy monitor, which is based on photoionization of a rare gas at low particle density (similar to [19]). We observe a clear linear relationship between the two quantities, which corroborates our approach.

This conclusion is further confirmed by Fig. 3(b): the XUV pulse energy and the THz amplitude are compared for several thousand XUV pulses and follow the same evolution. The observed correlation between the THz amplitudes and measured XUV pulse energies yields a (relative) standard deviation of ±2 μJ. We thereby demonstrate that STEs can measure pulse energies as low as a few μJ, and it has been shown that STEs can work in the linear regime up to few mJ pulse energies when operated below a fluence of a few mJ/cm^2 [29]. In comparison to the FERMI XUV pulse energy monitor, STEs provide a similar pulse energy range over which they can be operated although with a larger error bar. Furthermore, while a calibration would be needed to provide absolute energies, STE-based energy monitors would provide a

direct measurement of the pulse energy at the sample, as opposite to ionization monitors, which are typically separated from the experimental chambers by several optical components. Therefore, our scheme also emerges as a robust and simple alternative technology to detect pulse energy fluctuations directly in the experimental end-station.

We note that arrival time measurements were in principle possible down to pulse energies of 5 μJ, which corresponds to about 10% of the typical pulse energies available from FERMI in this wavelength range [see Fig. 3(a)]. We observe a scaling of the timing jitter from below 10 fs for pulse energies larger than 25 μJ to below 30 fs for pulse energies below 10 μJ. This increase may stem from the smaller THz signal levels, which may lead to a decreased precision of our technique (see Supplement 1).

C. Pulse Duration Monitoring

Figure 4 shows a typical THz waveform and the corresponding spectrum as detected for pump pulses with 30 fs duration and a
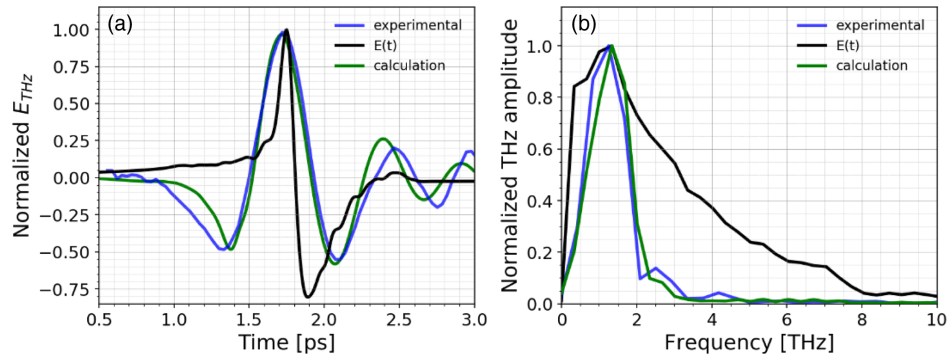
Fig. 4. THz waveform generated by 30 fs pulses at a wavelength of 20 nm: (a) time-domain THz wave form and (b) corresponding THz spectrum as derived from the experiment (blue), simulation neglecting the transfer functions of the sapphire substrate and the 2 mm ZnTe crystal (black), and simulation including the transfer function of the 2 mm ZnTe crystal (green).
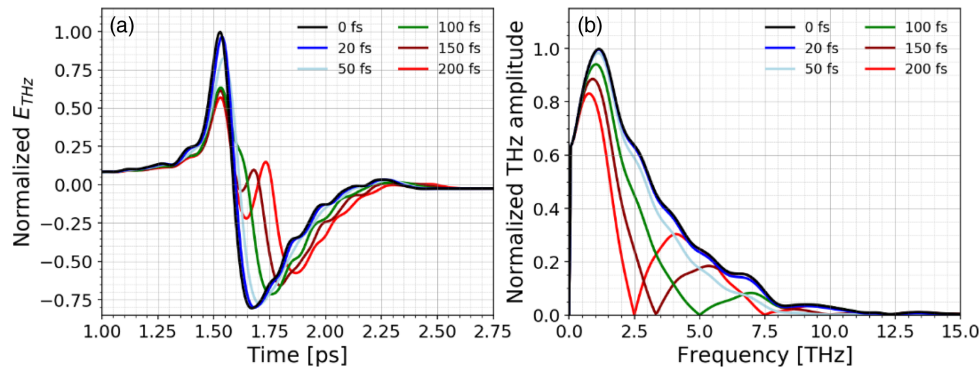

Fig. 5. Calculated THz waveforms for excitation by two subsequent 30 fs pulses with various pulse–pulse delays at a wavelength of 20 nm: (a) time-domain waveforms and (b) THz amplitude spectra assuming different separation of two XUV pulses.

wavelength of 20 nm. The shape of the generated THz pulse is determined by the intensity profile of the pump pulse, not the actual electric field [30] (Supplement 1, Fig. S5), which can hence be determined by monitoring the THz waveform and spectrum.

One can simulate the experimentally derived THz electric field [black curve in Fig. 4(a)] by convoluting the emitted THz electric field directly behind the metal stack for a 10 fs pump pulse, which was determined in a previous experiment, with the respective x-ray pulse envelope [28]. Note that the signal waveform measured by electro-optic sampling is affected by the frequency-dependent transfer function of the setup and the electro-optic sampling process. Once these influences are accounted for, good agreement between experiment and simulation is achieved (see Fig. 4 and Supplement 1).

This example demonstrates that the detection of the THz pulse is strongly limited by the detection system used in this experiment and that the true spectrum of the emitted THz pulse is much broader. Our simulations indicate that by using a sufficiently broadband detection setup, an XUV pulse duration of below 50 fs (see Supplement 1, Fig. S5) can be monitored by detecting the THz waveform by the STE.

For experiments exploiting the high intensity of current FELs (e.g., nonlinear studies), the structure of each individual x-ray/XUV pulse becomes significant. At the XUV FEL FLASH, it has been observed by the THz streaking technique that roughly 10% of the pulses consist of two or more distinct peaks [31]. As shown in Fig. 5, our technique should be well capable to observe such fine structure down to the level of a few 10 fs.

4. DISCUSSION

We have demonstrated experimentally that the arrival time of XUV FEL pulses can be clocked by single-shot electro-optic sampling of THz pulses generated by optical rectification in an STE, and that the relative energy of each XUV pulse can be monitored by the amplitude of the corresponding emitted THz pulse. We also showed that the emitted THz waveform is indicative of the XUV pulse duration and even its fine structure. Our scheme, therefore, provides access to many important properties of XUV/x-ray FEL pulses at once. The encoding of the XUV pulse properties into THz pulses opens up the possibility to monitor arrival time, pulse duration, and pulse energy of individual x-ray pulses at MHz repetition rates in a cost-efficient and robust way by utilizing established single-shot electro-optic detection techniques, which are already in routine operation at large-scale photon science facilities [27,32].

The precision of the arrival time measurement depends on the XUV pulse energy and on the specific design of the spectral decoding scheme (see Supplement 1). In our experiments, we demonstrate that a value of below 10 fs can be achieved with our prototype setup for XUV pulse energies above 25 µJ. This value compares well with operational arrival time monitors, e.g., at the European XFEL [33,34]. We currently investigate, whether there is a fundamental limit for the precision given by the THz generation process in the STE. Further improvement of the arrival time precision can also be expected from increasing the detection bandwidth and signal-to-noise ratio.

The potential for the determination of relative pulse energies needs to be further explored. The current implementation of our scheme will not rival the precision of the successfully routinely employed gas monitor detectors [19] but can provide convenient access to the x-ray pulse energies directly in or behind the experiment.

The capabilities of our scheme to determine pulse duration and fine structures within the pulses are currently limited by our choice of the electro-optic crystal to about 200 fs. Note that for broadband THz pulses, the electro-optic response of the detection crystal will have spectral dips with lower sensitivity, which might partially blind the detection system. Currently, detection crystals with different absorption bands are known [35,36]. Depending on the specific demand and spectral range of interest, the most suitable crystal should be chosen. Also, the detection bandwidth can be increased by improving the temporal resolution of the single-shot electro-optic detection setup. In this context, alternative implementations of electro-optic single-shot detection schemes or appropriate numerical retrieval techniques that provide a better temporal resolution should be considered (see, e.g., [37–40]). While more elaborate concepts such as THz streaking [13,14,41] still achieve superior precision and accuracy, our demonstrated methodology has the advantage of being considerably less complex with large potential for future improvements.

Fundamentally, the time resolution of our approach with respect to pulse duration is given by the response time of our STE, which is predominantly determined by the electron-spin relaxation time of the ferromagnetic layer and amounts to approximately 100 fs [28]. By a proper deconvolution procedure [42] and sufficient signal-to-noise ratio, we expect that the time resolution can be reduced to several 10 fs.

This study is also interesting from a fundamental scientific viewpoint. The applicability of our scheme has been verified at wavelengths of 20 and 29 nm. We did not observe noticeable differences in the efficiency of the spintronic THz emission process between the two wavelengths. According to our current understanding of the working principle of the STE, it is only relevant that the pump pulse deposits energy as fast as possible in the electronic system of the ferromagnet, regardless of the specific photon energy [28,30,43]. Our experiments indicate that this notion extends to even an order of magnitude larger photon energies than used previously [30,43]. It is consistent with works that did not observe a noticeable impact of the pump-photon energy from XUV to the visible [44] to the THz range [42] on ultrafast demagnetization, which has the same driving force as ultrafast spin transport [28].

We note that the penetration depth at the wavelengths utilized in our experiments is between 10 and 20 nm. Therefore, over 40% of the incident XUV energy is absorbed in the STE. As absorption coefficients generally decrease in the x-ray regime, a drop in deposited energy and, thus, in THz emission, can be expected. However, we believe that by choosing appropriate absorber materials and layer stack designs, e.g., by considering characteristic core-level absorption edges, our scheme should be applicable also in the soft and harder x-ray regime.

If the aforementioned absorption loss in metallic layers is endurable, STEs grown on SiN or SiC membranes can be envisioned as an online monitor in the direct beamline in front of the experiment if the heat management in the thin substrate is accomplished. Apart from that, STEs on solid substrates, which typically absorb all of the XUV energy, may find their application behind certain gas phase experiments that leave the XUV pulse properties largely unperturbed. Another option is to combine STEs on solid substrates with online XUV grating spectrometers such as the variable line spacing (VLS) spectrometer in operation at the FLASH FEL [45] and perform the XUV pulse characterization on a higher diffraction order.

In conclusion, our study establishes spintronic THz sources as ultrafast versatile photodiodes operative from the infrared to the XUV regime with large potential for future improvements in terms of arrival time and pump-pulse energy resolution.

Disclosures. T.S.S. and T.K. are shareholders of TeraSpinTec GmbH, and T.S.S. is an employee of TeraSpinTec GmbH.

Data availability. Data underlying the results presented in this paper are not publicly available at this time but may be obtained from the authors upon reasonable request.

Supplemental document. See Supplement 1 for supporting content.

[†]These authors contributed equally to this work.

REFERENCES

1. C. Pellegrini, "X-ray free-electron lasers: from dreams to reality," Phys. Scripta **T169**, 014004 (2016).
2. W. Decking, S. Abeghyan, P. Abramian, *et al.*, "A MHz-repetition-rate hard x-ray free-electron laser driven by a superconducting linear accelerator," Nat. Photonics **14**, 391–397 (2020).
3. A. Halavanau, F.-J. Decker, C. Emma, J. Sheppard, and C. Pellegrini, "Very high brightness and power LCLS-II hard x-ray pulses," J. Synchrotron Rad. **26**, 635–646 (2019).
4. M. Dunne, "X-ray free-electron lasers light up materials science," Nat. Rev. Mater. **3**, 290 (2018).
5. V. Marx, "Structural biology: doors open at the European XFEL," Nat. Methods **14**, 843–846 (2017).
6. P. Fromme, "XFELs open a new era in structural chemical biology," Nat. Chem. Biol. **11**, 895 (2015).
7. A. L. Cavalieri, D. M. Fritz, S. H. Lee, *et al.*, "Clocking femtosecond x rays," Phys. Rev. Lett. **94**, 114801 (2005).
8. A. Azima, S. Düsterer, P. Radcliffe, H. Redlin, N. Stojanovic, W. Li, H. Schlarb, J. Feldhaus, D. Cubaynes, M. Meyer, J. Dardis, P. Hayden, P. Hough, V. Richardson, E. T. Kennedy, and J. T. Costello, "Time-resolved pump-probe experiments beyond the jitter limitations at FLASH," Appl. Phys. Lett. **94**, 144102 (2009).
9. C. Gahl, A. Azima, M. Beye, M. Deppe, K. Döbrich, U. Hasslinger, F. Hennies, A. Melnikov, M. Nagasono, A. Pietzsch, M. Wolf, W. Wurth, and A. Föhlisch, "A femtosecond x-ray/optical cross-correlator," Nat. Photonics **2**, 165–169 (2008).
10. F. Tavella, N. Stojanovic, G. A. Geloni, and M. Gensch, "Few femtosecond timing at 4th generation x-ray light sources," Nat. Photonics **5**, 162–165 (2011).
11. M. R. Bionta, N. Hartmann, M. Weaver, D. French, D. J. Nicholson, J. P. Cryan, J. M. Glownia, K. Baker, C. Bostedt, M. Chollet, Y. Ding,

D. M. Fritz, A. R. Fry, D. J. Kane, J. Krzywinski, H. T. Lemke, M. Messerschmidt, S. Schorb, D. Zhu, W. E. White, and R. N. Coffee, "Spectral encoding method for measuring the relative arrival time between x-ray/optical pulses," Rev. Sci. Instrum. **85**, 083116 (2014).

12. M. B. Danailov, F. Bencivenga, F. Capotondi, F. Casolari, P. Cinquegrana, A. Demidovich, E. Giangrisostomi, M. P. Kiskinova, M. Kurdi, M. Manfredda, C. Masciovecchio, R. Mincigrucci, I. P. Nikolov, E. Pedersoli, E. Principi, and P. Sigalotti, "Towards jitter-free pump-probe measurements at seeded free electron laser facilities," Opt. Express **22**, 12869–12879 (2014).

13. U. Frühling, M. Wieland, M. Gensch, T. Gebert, B. Schütte, M. Krikunova, R. Kalms, F. Budzyn, O. Grimm, J. Rossbach, E. Plönjes, and M. Drescher, "Singleshot THz field driven x-ray streak-camera," Nat. Photonics **3**, 523–528 (2009).

14. I. Grguraš, A. R. Maier, C. Behrens, T. Mazza, T. J. Kelly, P. Radcliffe, S. Düsterer, A. K. Kazansky, N. M. Kabachnik, T. Tschentscher, J. T. Costello, M. Meyer, M. C. Hoffmann, H. Schlarb, and A. L. Cavalieri, "Ultrafast x-ray pulse characterization at free-electron lasers," Nat. Photonics **6**, 852–857 (2012).

15. R. Riedel, A. Al-Shemmary, M. Gensch, T. Golz, M. Harmand, N. Medvedev, M. J. Prandolini, K. Sokolowski-Tinten, S. Toleikis, U. Wegner, B. Ziaja, N. Stojanovic, and F. Tavella, "Single-shot pulse duration monitor for extreme ultraviolet and x-ray free-electron lasers," Nat. Commun. **4**, 1731 (2013).

16. P. Finetti, H. Höppner, E. Allaria, *et al.*, "Pulse duration of seeded free-electron lasers," Phys. Rev. X **7**, 021043 (2017).

17. J. Duris, S. Li, T. Driver, *et al.*, "Tunable isolated attosecond x-ray pulses with gigawatt peak power from a free-electron laser," Nat. Photonics **14**, 30–36 (2020).

18. M. Wieland, N. M. Kabachnik, M. Drescher, Y. Deng, Y. Arbelo, N. Stojanovic, B. Steffen, J. Roensch-Schulenburg, R. Ischebeck, A. Malyzhenkov, E. Prat, and P. Juranić, "Deriving x-ray pulse duration from center-of-energy shifts in THz-streaked ionized electron spectra," Opt. Express **29**, 32739–32754 (2021).

19. M. Richter, A. Gottwald, U. Kroth, A. A. Sorokin, S. V. Bobashev, L. A. Shmaenok, J. Feldhaus, C. Gerth, B. Steeg, K. Tiedtke, and R. Treusch, "Measurement of gigawatt radiation pulses from a vacuum and extreme ultraviolet free-electron laser," Appl. Phys. Lett. **83**, 2970 (2003).

20. H. Yoneda, K. Tokuyama, K.-I. Ueda, H. Yamamoto, and K. Baba, "High-power terahertz radiation emitter with a diamond photoconductive switch array," Appl. Opt. **40**, 6733–6736 (2001).

21. S. Ono, H. Murakami, A. Quema, G. Diwa, N. Sarukura, R. Nagasaka, Y. Ichikawa, H. Ogino, E. Ohshima, A. Yoshikawa, and T. Fukuda, "Generation of terahertz radiation using zinc oxide as photoconductive material excited by ultraviolet pulses," Appl. Phys. Lett. **87**, 261112 (2005).

22. X. Ropagnol, Z. Kovács, B. Gilicze, M. Zhuldybina, F. Blanchard, C. M. Garcia-Rosas, S. Szatmári, I. B. Földes, and T. Ozaki, "Intense sub-terahertz radiation from wide-bandgap semiconductor based large-aperture photoconductive antennas pumped by UV lasers," New J. Phys. **21**, 113042 (2019).

23. T. Seifert, S. Jaiswal, U. Martens, J. Hannegan, L. Braun, P. Maldonado, F. Freimuth, A. Kronenberg, J. Henrizi, I. Radu, E. Beaurepaire, Y. Mokrousov, P. M. Oppeneer, M. Jourdan, G. Jakob, D. Turchinovich, L. M. Hayden, M. Wolf, M. Münzenberg, M. Kläui, and T. Kampfrath, "Efficient metallic spintronic emitters of ultrabroadband terahertz radiation," Nat. Photonics **10**, 483–488 (2016).

24. T. Seifert, S. Jaiswal, M. Sajadi, G. Jakob, S. Winnerl, M. Wolf, M. Kläui, and T. Kampfrath, "Ultrabroadband single-cycle terahertz pulses with peak fields of 300 kV cm^{-1} from a metallic spintronic emitter," Appl. Phys. Lett. **110**, 252402 (2017).

25. J. A. Fülöp, S. Tzortzakis, and T. Kampfrath, "Review: laser-driven strong-field terahertz sources and their novel applications," Adv. Opt. Mater. **8**, 1900681 (2020).

26. Z. Jiang and X.-C. Zhang, "Electro-optic measurement of THz field pulses with a chirped optical beam," Appl. Phys. Lett. **72**, 1945 (1998).

27. S. Kovalev, B. Green, T. Golz, S. Maehrlein, N. Stojanovic, A. S. Fisher, T. Kampfrath, and M. Gensch, "Probing ultra-fast processes with high dynamic range at 4th-generation light sources: arrival time and intensity binning at unprecedented repetition rates," Struct. Dyn. **4**, 024301 (2017).

28. R. Rouzegar, R. Rouzegar, L. Brandt, L. Nadvornik, D. A. Reiss, A. L. Chekhov, O. Gueckstock, C. In, M. Wolf, T. S. Seifert, P. W. Brouwer, G. Woltersdorf, and T. Kampfrath, "Laser-induced terahertz spin transport in magnetic nanostructures arises from the same force as ultrafast demagnetization," arXiv:2103.11710 (2021).

29. T. Vogel, A. Omar, S. Mansourzadeh, F. Wulf, N. M. Sabanés, M. Müller, T. S. Seifert, A. Weigel, G. Jakob, M. Kläui, I. Pupeza, T. Kampfrath, and C. J. Saraceno, "Average power scaling of THz spintronic emitters in reflection geometry," arXiv:2112.09582 (2022).

30. R. I. Herapath, S. M. Hornett, T. S. Seifert, G. Jakob, M. Kläui, J. Bertolotti, T. Kampfrath, and E. Hendry, "Impact of pump wavelength on terahertz emission of a cavity-enhanced spintronic trilayer," Appl. Phys. Lett. **114**, 041107 (2019).

31. U. Frühling, "Light-field streaking for FELs," J. Phys. B **44**, 243001 (2011).

32. M. Chen, J.-C. Deinert, B. Green, Z. Wang, I. Ilyakov, N. Awari, M. Bawatna, S. Germanskiy, T. V. A. G. de Oliveira, G. Geloni, T. Tanikawa, M. Gensch, and S. Kovalev, "Pulse- and field-resolved THz-diagnostics at 4th generation light sources," Opt. Express **27**, 32360–32369 (2019).

33. H. J. Kirkwood, R. Letrun, T. Tanikawa, *et al.*, "Initial observations of the femtosecond timing jitter at the European XFEL," Opt. Lett. **44**, 1650–1653 (2019).

34. T. Sato, R. Letrun, H. J. Kirkwood, *et al.*, "Femtosecond timing synchronization at megahertz repetition rates for an x-ray free electron laser," Optica **7**, 716–717 (2020).

35. A. Leitenstorfer, S. Hunsche, J. Shah, M. C. Nuss, and W. H. Knox, "Detectors and sources for ultrabroadband electro-optic sampling-experiment and theory," Appl. Phys. Lett. **74**, 1516 (1999).

36. I. E. Ilyakov, G. Kh. Kitaeva, B. V. Shishkin, and R. A. Akhmedzhanov, "The use of DSTMS crystal for broadband terahertz electro-optic sampling based on laser pulse amplitude changes," Laser Phys. Lett. **15**, 125401 (2018).

37. J. Shan, A. S. Weling, E. Knoesel, L. Bartels, M. Bonn, A. Nahata, G. A. Reider, and T. F. Heinz, "Single-shot measurement of terahertz electromagnetic pulses by use of electro-optic sampling," Opt. Lett. **25**, 426–428 (2000).

38. Y. Minami, Y. Hayashi, J. Takeda, and I. Katayama, "Single-shot measurement of a terahertz electric waveform using a reflective echelon mirror," Appl. Phys. Lett. **103**, 051103 (2013).

39. D. A. Walsh, E. W. Snedden, and S. P. Jamison, "The time resolved measurement of ultrashort terahertz-band electric fields without an ultrashort probe," Appl. Phys. Lett. **106**, 181109 (2015).

40. E. Roussel, C. Szwaj, C. Evain, B. Steffen, C. Gerth, B. Jalali, and S. Bielawski, "Phase diversity electro-optic sampling: a new approach to single-shot terahertz waveform recording," Light Sci. Appl. **11**, 14 (2022).

41. R. Ivanov, I. J. B. Macias, J. Liu, G. Brenner, J. Roensch-Schulenburg, G. Kurdi, U. Frühling, K. Wenig, S. Walther, and A. Dimitriou, "Single-shot temporal characterization of XUV pulses with duration from ∼10 fs to ∼350 fs at FLASH," J. Phys. B **53**, 184004 (2020).

42. A. L. Chekhov, Y. Behovits, J. J. F. Heitz, C. Denker, D. A. Reiss, M. Wolf, M. Weinelt, P. W. Brouwer, M. Münzenberg, and T. Kampfrath, "Ultrafast demagnetization of iron induced by optical versus terahertz pulses," Phys. Rev. X **11**, 041055 (2021).

43. E. Th. Papaioannou, G. Torosyan, S. Keller, L. Scheuer, M. Battiato, V. K. Mag-Usara, J. L'huillier, M. Tani, and R. Beigang, "Efficient terahertz generation using Fe/Pt spintronic emitters pumped at different wavelengths," IEEE Trans. Magn. **54**, 9100205 (2018).

44. M. Schneider, B. Pfau, C. M. Günther, C. von Korff Schmising, D. Weder, J. Geilhufe, J. Perron, F. Capotondi, E. Pedersoli, M. Manfredda, M. Hennecke, B. Vodungbo, J. Lüning, and S. Eisebitt, "Ultrafast demagnetization dominates fluence dependence of magnetic scattering at Co *M* edges," Phys. Rev. Lett. **125**, 127201 (2020).

45. G. Brenner, S. Kapitzkia, M. Kuhlmann, E. Ploenjes, T. Noll, F. Siewert, R. Treusch, K. Tiedtke, R. Reininger, M. D. Roper, M. A. Bowler, F. M. Quinn, and J. Feldhaus, "First results from the online variable line spacing grating spectrometer at FLASH," Nucl. Instrum. Methods Phys. Res., Sect. A **635**, S99–S103 (2011).